Metal Loaded Zeolite Adsorbents for Phosphine Removal

Wen-Chih Li,[†] Hsunling Bai,*[,†] Jung-Nan Hsu,[†,‡] Shou-Nan Li,[‡] and Chienchih Chen[†]

Institute of Environmental Engineering, National Chiao Tung University, Hsinchu, Taiwan, and Energy and Environment research Laboratories, Industrial Technology Research Institute, Hsinchu, Taiwan

Phosphine (PH_3) is a highly toxic air pollutant commonly used in the semiconductor and optoelectronic industries, but it has received less research attention due to its handling difficulty. In this study, metal (Cu, Zn, or Mn) loaded ZSM-5 and Y zeolite adsorbents are first prepared for the adsorption of PH_3 toxic gas. The physical and chemical properties of the adsorbents which influence the PH_3 adsorption capacity are analyzed. The results show that >99% PH_3 adsorption efficiency is achieved when zeolites are loaded with Cu. The maximal PH_3 adsorption capacities are about the same for both zeolites at 1.9 mol of PH_3/mol of Cu, which occurs at similar Cu loaded mass of 3.0−3.5%, beyond which the decrease in specific surface area is the major factor responsible for the decrease of PH_3 adsorption capacity. The maximum adsorption capacity per loaded metal mass is much higher than literature data using CuO only for adsorbing hydride gases.

1. Introduction

The hydride gas of phosphine (PH_3) is commonly used in the fabricating processes of the semiconductor and optoelectronic industries.[1] It is a hazardous air pollutant and must be immediately abated by local scrubbers installed after process equipment. Various methods have been used for gaseous hydride removal such as combustion, gas−liquid reaction, and dry adsorption.[2,3] Hardwick and Mailloux[2] indicated that oxidizing hydride gas by combustion can be costly while aqueous treatment tends to generate large volumes of dilute aqueous waste. On the other hand, carbon dry adsorption would be less expensive, simpler to operate, and involve fewer waste disposal problems than the wet scrubber method.[4,5] However, it has suffered from its inflammability.[2,6,7] When large quantities of spent carbon react exothermically with air, spontaneous combustion might occur; thus the activated carbon adsorbent is not practically acceptable in abating the toxic hydride gases for the semiconductor and optoelectronic industries.

On the other hand, zeolite materials are characterized by their high surface area, large pore volume, and high thermal stability.[6] Zeolite has been studied for the removal of volatile organic compounds (VOCs),[7,8] and it has gradually substituted for activated carbon in reducing VOC emissions from the semiconductor and optoelectronic industries.[9] However, research on the possibility of abating any hydride gas by zeolite dry adsorption has never been studied.

Ion-exchange and impregnation methods which combine zeolite supports and active metals have been frequently used for the preparation of catalysts or adsorbents. The effects of types and amounts of metals on the activities of the zeolite adsorbents or catalysts have been investigated in removing air contaminants such as VOCs and NOx.[8,10−13] However, there has been limited research aimed at the relationship between adsorbent capacity and the physical/chemical characteristics of the adsorbents.

In this study, two types of zeolite, ZSM-5 and Y zeolites, were loaded with metals (Zn, Mn, and Cu) to act as chemical adsorbents and their performance for removing PH_3 from a gas stream was compared. The correlation between the physical/chemical properties of adsorbents and their PH_3 adsorption capacities was then discovered.

2. Experimental Section

2.1. Zeolite Adsorbents. Two commercial zeolites (Zeolyst, Valley Forge, PA), ZSM-5 (CBV5524G) and Y (CBV500) zeolites, were used as supported materials of metal adsorbents. The BET surface area, pore size, and pore volume of the adsorbents were measured by a surface analyzer with nitrogen adsorption (Micromeritics ASAP 2020). Table 1 compares the physical and chemical properties of these two zeolites prior to the metal loading process. Although the measured data are somewhat different from those provided by the manufacturer, it is observed that Y zeolite has a higher BET surface area than the ZSM-5 zeolite. The measured BET surface area and pore volume for Y zeolite are 641 m^2/g and 0.36 cm^3/g, respectively, and 388 m^2/g and 0.23 cm^3/g for ZSM-5 zeolite. As for the pore size, because the surface analyzer can measure only down to 2 nm of pore size, only the mesopore size is reported here. The mesopore size of Y zeolite, 2.22 nm, is slightly smaller than that of ZSM-5 zeolite, 2.36 nm. The channel sizes of Y zeolite and ZSM-5 zeolite are around 7.4 × 7.4 and 5.3 × 5.6 Å, as cited directly from literature data.[14] Moreover, ZSM-5 is a high silica zeolite with a SiO_2/Al_2O_3 molar ratio of 50 as provided by the manufacturer, while the Y zeolite has a SiO_2/Al_2O_3 molar ratio of only 5.2.

A total of 10 g of each type of zeolite and 250 mL of metal precursor, either $Cu(NO_3)_2 \cdot 3H_2O$, $Zn(NO_3)_2 \cdot 6H_2O$, or $Mn(CH_3COO)_2 \cdot 4H_2O$, were stirred individually at room temperature for 12 h. After filtration and washing process, the adsorbents were dried in an oven at 120 °C for 12 h and then calcined in a furnace at 550 °C for 6 h. The amount of metal loaded on the zeolite was varied by using different concentrations of metal precursor solutions, and the actual mass of metal loaded on the zeolite was determined by inductively coupled plasma atomic emission spectrometry (ICP-AES, Jarrell Ash).

The maximum $Cu(NO_3)_2$ concentration of 5 M used in this study is approaching its saturated concentration (~5.27 M); therefore, multiple metal loading[10,15] was applied for the ZSM-5 sample in order to achieve a higher copper loading. The ZSM-5 zeolite was immersed in a $Cu(NO_3)_2$ concentration of 5 M for 12 h at room temperature first. Then after filtration, washing,

* To whom correspondence should be addressed. Tel.: +886-3-573-1868. Fax: +886-3-572-5958. E-mail: hlbai@mail.nctu.edu.tw.

[†] National Chiao Tung University

[‡] Industrial Technology Research Institute

10.1021/ie071074n CCC: $40.75
Published on Web 01/23/2008

Table 1. Physical and Chemical Properties of Zeolites Used in This Study

zeolite type	BET surf. area (m^2/g)	pore vol (cm^3/g)	Na_2O fraction (% w/w)	SiO_2/Al_2O_3 (molar ratio)
ZSM-5	388 (425[a])	0.23	0.05[a]	50[a]
Y	641 (750[a])	0.36	0.02[a]	5.2[a]

[a] Data were provided by the manufacturer.

and drying, the zeolite sample was immersed again in a 5 M $Cu(NO_3)_2$ solution under the same procedure. Finally, the double loaded zeolite sample was calcined at 550 °C for 6 h.

2.2. PH_3 Adsorption. The PH_3 adsorption experiments were carried out in a chamber that controls pressure to be slightly below atmospheric pressure for avoiding PH_3 toxic gas escaping from the adsorption column. The adsorption temperature was at ambient temperature of 25 ± 1 °C. The adsorption column was stainless steel with 2.25 cm inner diameter and 11.7 cm in length. A total of 10 g of adsorbents was packed into it during each test. Because PH_3 burns readily in air and leads to a safety problem, 1% (v/v) PH_3 gas was supplied from a cylinder in He inert gas with a flow rate of 0.2 L/min being regulated by a mass flow controller (BROOKS 5850E). Fourier transform infrared spectrometry (FTIR, MIDAC) was used to continuously monitor the concentration of PH_3. An additional adsorber was placed before exhausting the waste gas to the atmosphere. The effective adsorption capacity was determined by the accumulated amount of adsorbed PH_3 during the period of over 99% PH_3 removal efficiency. That is, the breakthrough point of the adsorbent was set at PH_3 effluent gas concentration of 0.01% (v/v).

Because PH_3 is a highly toxic compound, any residual PH_3 remaining in the system as gas-phase molecules or being adsorbed on the adsorbent could result in a human health problem. Therefore, after the completion of the adsorption test, the whole adsorption system was purged by a N_2 gas flow to remove PH_3 gaseous residue. Also, external air of reverse direction was passed through the adsorption column to fully ensure oxidization of the adsorbed PH_3 on the metal/zeolite adsorbents.

3. Results and Discussion

3.1. Blank Test and Selection of Metal Species for PH_3 Removal. The PH_3 removal efficiency and adsorption capacity were tested for the ZSM-5 and Y zeolites prior to metal loading. The results showed that, although ZSM-5 zeolite achieved a relatively higher PH_3 removal efficiency (with the best efficiency at 97%) than that of the Y zeolite (best at 73%), they still could not reach the goal of over 99% PH_3 removal. Hence one can say that blank tests of both zeolite materials are not effective in the PH_3 adsorption and thus a metal precursor must be incorporated with zeolites for effective PH_3 removal.

Three metal precursors, $Cu(NO_3)_2 \cdot 3H_2O$, $Zn(NO_3)_2 \cdot 6H_2O$, and $Mn(CH_3COO)_2 \cdot 4H_2O$, with a concentration of 1.0 M (moles per liter) were evaluated for their PH_3 adsorption efficiencies on the zeolite adsorbents, and the results are shown in Figure 1 for Y zeolite. One can see that the PH_3 removal efficiency for Cu loaded zeolite adsorbent is much higher than those of Zn and Mn loaded zeolites. The PH_3 removal efficiency abated by the Cu/Y zeolite adsorbent can be over 99%, but the maximum PH_3 removal efficiencies are only 84% and 80%, respectively, for Zn/zeolite and Mn/zeolite adsorbents. In addition, the high PH_3 removal efficiency can last for a much longer period for Cu/zeolite adsorbent. Therefore, Cu is chosen as the metal species for later study.

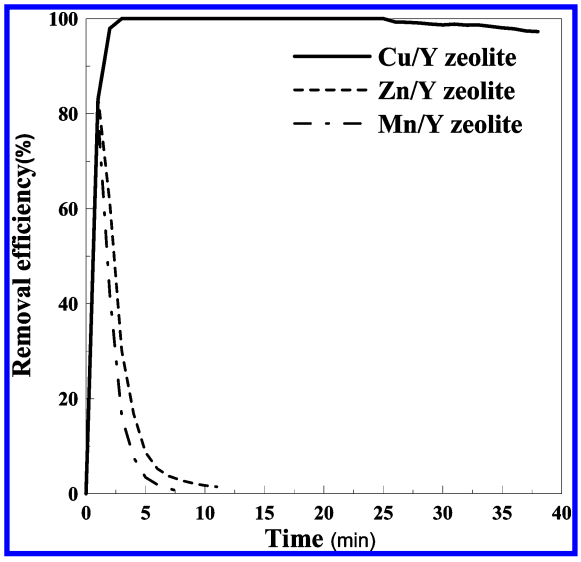

Figure 1. Comparison of removal efficiencies of Cu, Zn, and Mn metal precursors loaded on Y zeolite adsorbents.

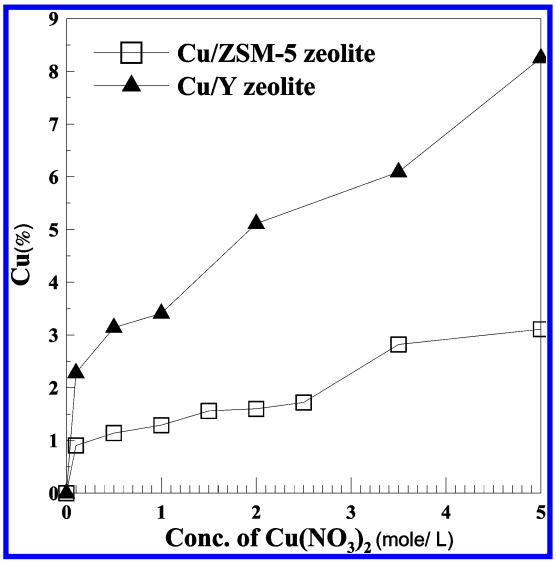

Figure 2. Cu loaded content (% by weight) on ZSM-5 and Y zeolite adsorbents as a function of $Cu(NO_3)_2$ precursor concentrations.

3.2. Characterization of Cu/Zeolite Adsorbents. Copper nitrate solutions of various concentrations ranging from 0.1 to 5.0 M were used to obtain Cu/zeolite adsorbents of various metal loading amounts. The relationships between the precursor concentration of $Cu(NO_3)_2$ and the actual loading amounts of Cu metal for both ZSM-5 and Y zeolite adsorbents are shown in Figure 2. It is observed that, as the $Cu(NO_3)_2$ precursor concentration is increased, the increasing rate of actual Cu content loaded on the Y zeolite is much higher than that on the ZSM-5 zeolite. The maximum Cu loadings on Y and ZSM-5 zeolites are 8.25% (w/w) and 3.11% (w/w), respectively, with a $Cu(NO_3)_2 \cdot 3H_2O$ precursor concentration of 5.0 M. This may be due to both relatively higher Al content of Y zeolite available for Cu ion exchange and higher BET surface area (pore volume), which provide more impregnation sites for Cu.

The variations in the BET surface area and pore volume of both Cu/ZSM-5 and Cu/Y zeolite adsorbents with respect to their actual Cu loaded mass (percent) are shown in Figure 3. One can see that the variations of the BET specific surface area (S_{BET}) for both Cu/zeolite and Cu/Y zeolite adsorbents are in trends similar to the variations of their pore volumes (V_{Total}). The BET specific surface area and pore volume of Cu/Y zeolite

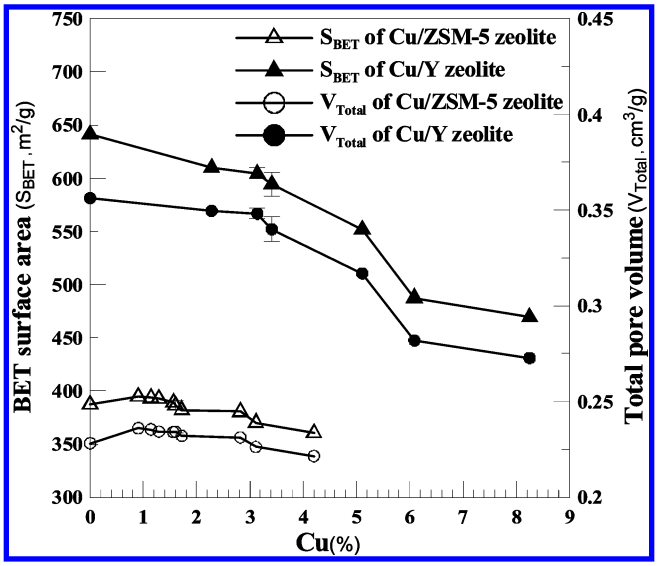

Figure 3. Variations in BET specific surface area and pore volume of adsorbents as a function of Cu loaded content (% by weight) for Cu/ZSM-5 and Cu/Y zeolite adsorbents. The maximal Cu loaded on ZSM-5 zeolite was 3.11% via single loading procedure; the sample with Cu mass concentration of 4.2% was from double loading procedure.

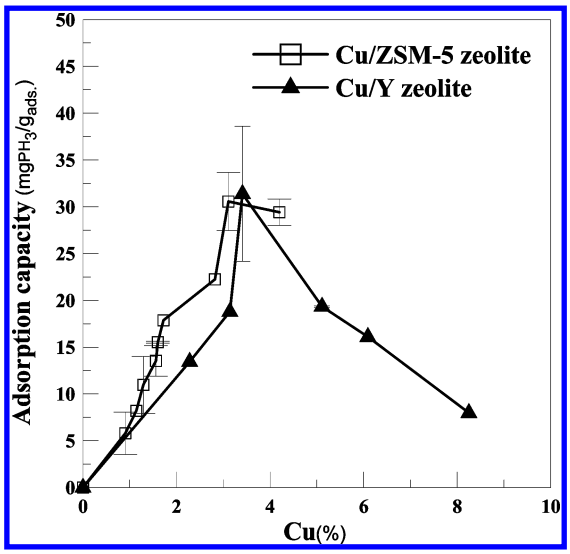

Figure 4. PH_3 adsorption capacity of Cu/ZSM-5 and Cu/Y zeolite adsorbents as a function of Cu loaded content (% by weight).

adsorbents decreased significantly from 641 to 469 m^2/g when the actual Cu loaded concentration was increased from 0 to 8.25% (w/w). For Cu/ZSM-5 zeolite adsorbents, their specific surface area and pore volume only change slightly either for single loaded Cu mass contents of up to 3.11% or after double Cu loading to a mass content of 4.2%. The changes in the BET specific surface area and pore volume of both types of zeolite adsorbents seem to match their Cu loaded amounts shown previously in Figure 2. Compared to the Y zeolite, ZSM-5 zeolite support has a much lower amount of Cu loading under the same precursor concentration. Therefore, the BET specific surface area does not change much for Cu/ZSM-5 zeolite adsorbents.

3.3. Adsorption Capacity. The effective adsorption capacities for achieving over 99% PH_3 removal with Cu/ZSM-5 and Cu/Y zeolite adsorbents are shown in Figure 4 as a function of actual Cu loaded mass concentration. As observed, the adsorption capacity of Cu/ZSM-5 zeolite adsorbent increases to 30.6 ± 3.0 mg of PH_3/g of adsorbent (mg/g_{ads}) as the Cu loaded concentration is increased to 3.11% (w/w). Although the Cu loading was enhanced from 3.11% to 4.20% (w/w) after double loading, the adsorption capacity of Cu/ZSM-5 zeolite adsorbent was even worse. Similarly, the adsorption capacity of Cu/Y zeolite adsorbent increases with increasing Cu loading and reaches its maximal value of 31.4 ± 7.0 mg/g_{ads} at a Cu loaded concentration of 3.42% (w/w); then it decreases as the Cu loaded concentration is further increased.

The very similar trend in the relationship between the adsorption capacity and the actual Cu loading for both Cu/ZSM-5 and Cu/Y zeolite adsorbents reveals that there is an optimal value of Cu loading of around 3.0−3.5% (w/w) no matter what type of zeolite adsorbent was used. The maximum adsorption capacity of 31 mg of PH_3/g of adsorbent for both types of Cu/zeolite adsorbents corresponds to an adsorption capacity of about 1 g of PH_3/g of Cu (∼1.9 mol of PH_3/mol of Cu). The maximum adsorption capacity per loaded metal mass obtained in this study is much higher than literature data using CuO for adsorbing hydride gases.[16,17] In the authors' prior study[17] on adsorbing SiH_4, the maximum adsorption capacity of only 0.15 mol of SiH_4/mol of CuO was observed with 40% (w/w) CuO supported on Al_2O_3 adsorbents. This may be due to that the surface area of the CuO/Al_2O_3 adsorbents[17] was only 121 m^2/g. To further clarify this, the relationship of the adsorption capacity with respect to the chemical/physical properties of Cu/zeolite samples is discussed in the following section.

3.4. PH_3 Adsorption Behaviors. For a better understanding of the PH_3 adsorption behaviors, the relationships of BET specific surface area and the adsorption capacity with respect to the Cu loading of the Cu/ZSM-5 zeolite adsorbent are shown in Figure 5a by their percentages relative to maximal values, i.e., 395 m^2/g and 30.6 mg/g_{ads}, respectively, for specific surface area and adsorption capacity. The BET surface area represents the physical adsorption properties of the adsorbent, while the actual Cu loading amount is the major chemical adsorption factor. It is seen clearly from Figure 5a that the adsorption capacity increases as the Cu loading is increased initially while the specific surface area changes only slightly with increasing Cu loading. At this stage the PH_3 adsorption is governed by the chemical factor of Cu content for Cu/ZSM-5 zeolite. However, as the Cu loading was further increased beyond 3.11% (w/w), the specific surface area of the zeolite decreased slightly and the adsorption capacity followed the decreasing trend of the specific surface area and decreased also.

The percentages relative to the maximum of BET surface area and effective adsorption capacity (i.e., 641 m^2/g and 31.4 mg/g_{ads}) as functions of Cu loading are shown in Figure 5b for the Cu/Y zeolite adsorbent. The adsorption capacity increases with increasing Cu loading mass, while the specific surface area slightly decreases to about 90% of its maximal value at Cu loading of 3.42% (w/w). This observation is very similar to that of Cu/ZSM-5 zeolite, as shown previously. However, as the Cu loading continuously increases to beyond ∼4% (w/w), the specific surface area of the Cu/Y zeolite decreases and the PH_3 adsorption capacity also decreases significantly. This indicates that the decrease of PH_3 adsorption capacity at higher Cu loading is mainly due to the loss of its specific surface area.

Therefore, from Figures 4, 5a, and 5b it is concluded that below 3.0−3.5% (w/w) of actual Cu loading, the chemical property (Cu content) dominates the available adsorption site, and beyond that the physical property (specific surface area or pore volume) is the major factor responsible for the PH_3 adsorption capacity. From Figures 2 and 4 it is known that ZSM-5 zeolite requires a much higher $Cu(NO_3)_2$ precursor

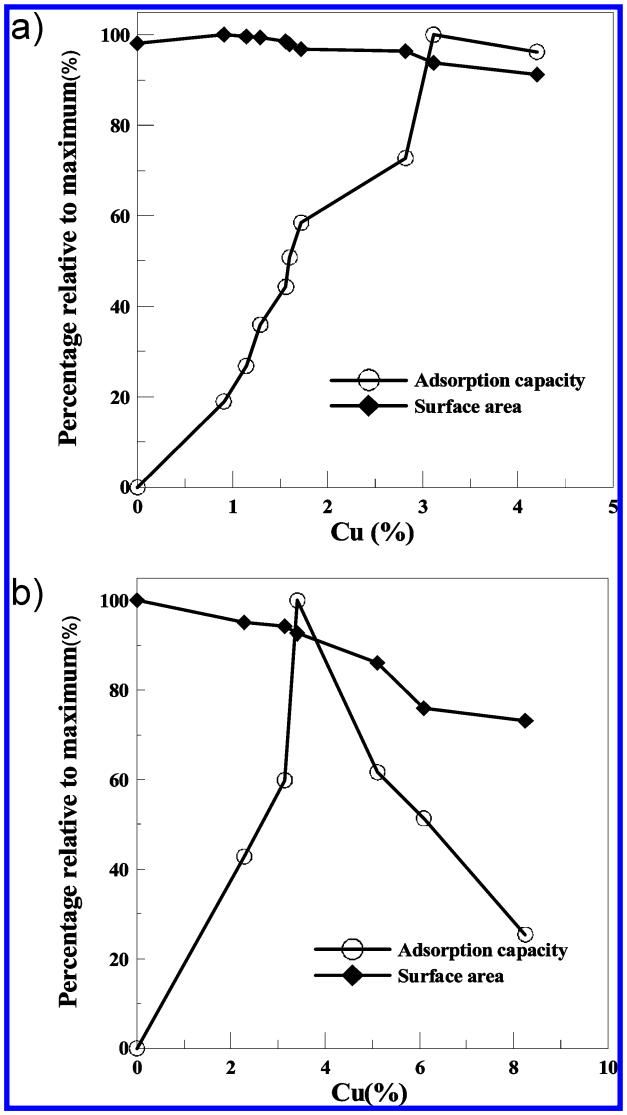

Figure 5. (a) Variations in percentages relative to maximal values of PH_3 adsorption capacity and specific surface area for Cu/ZSM-5 zeolite adsorbent as a function of Cu loaded content (% by weight). (b) Variations in percentages relative to maximal values of PH_3 adsorption capacity and specific surface area for Cu/Y zeolite adsorbent as a function of Cu loaded content (% by weight).

concentration (~5 mol/L) to reach this optimal Cu loading than Y zeolite does (~1 mol/L).

It is also interesting to evaluate whether the Cu loaded on zeolites is via ion exchange or impregnation processes. Although a quantitative analysis on the exact amount of ion-exchanged Cu was not performed, a qualitative analysis can be checked. Since the major metal species presented in both zeolites available for ion exchange is Na^+, based on the manufacturer's data, the mass fractions of Na_2O are 0.05% and 0.2% (w/w), respectively, for ZSM-5 and Y zeolites. This is relatively low compared to the optimal Cu loaded mass of around 3.0−3.5% (w/w) for achieving the maximum PH_3 adsorption capacity. Besides, in this study, a very high $Cu(NO_3)_2$ precursor concentration of up to 5 M was used, a value much larger than those typically employed for obtaining ion-exchanged Cu.[10] Therefore, the Cu loaded on the zeolites should be mainly from impregnation of Cu precursor.

3.5. X-ray Photoelectron Spectroscopic (XPS) Analysis. The chemical states of the elements on the Cu/ZSM-5 adsorbent before and after adsorption were examined by XPS. The core level binding energy of C 1s for carbon at 284.6 eV was used as an internal reference for calibration. The X-ray source was operated by an Al Kα anode with a photo energy of $h\nu = 1486.6$ eV. Figure 6 shows the XPS spectra of core level binding energy in Cu 2p before adsorption and after adsorption/oxidation. The XPS fitting data of the Cu peaks, the possible Cu statuses and their relative percentages, and the ratios of satellites accompanying the major Cu peak are summarized in Table 2. It must be noted that an XPS analysis of the adsorbent right after adsorption was not possible due to safety concerns; the XPS data were performed on Cu/zeolite after adsorption and air purging to ensure full oxidization of the adsorbed PH_3 on the metal/zeolite adsorbents.

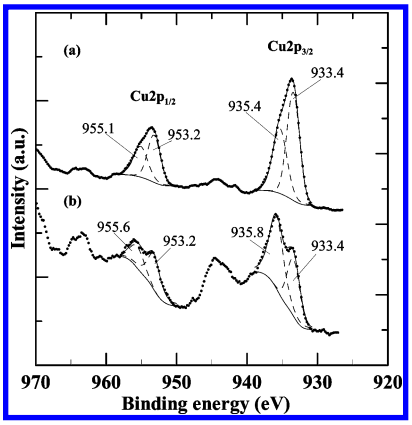

Figure 6. XPS spectra of Cu/ZSM-5 zeolite adsorbent for Cu 2p: (a) before PH_3 adsorption; (b) after PH_3 adsorption and air purging. The dots are the XPS measured data, the dashed curves are the split fittings of the XPS measured data, and the solid curves are the sum of each spectrum fitting value. The Cu/ZSM-5 zeolite was prepared by 1.0 M $Cu(NO_3)_2$ precursor concentration.

Table 2. XPS Data of the Cu 2p Spectra and Their Possible Cu Statuses Before and After PH_3 Adsorption

	before adsorption (freshly made zeolite)		after adsorption and air purging	
Cu status	CuO	$Cu(OH)_2$	CuO	$Cu(OH)_2$
binding energy of Cu $2p_{3/2}$ (eV)	933.4	935.4	933.4	935.8
binding energy of Cu $2p_{1/2}$ (eV)	953.2	955.1	953.2	955.6
fwhm (eV)	2.12	2.37	2.12	2.37
doublet separation (eV)	19.8	19.7	19.8	19.8
calculated Cu percentage (%)	57.3	42.7	45.6	54.4
ratio of satellite peak/Cu $2p_{3/2}$ (%)	6.6		33.3	
ratio of satellite peak/Cu $2p_{1/2}$ (%)	8.3		38.6	

As observed from Figure 6 and Table 2, the major Cu $2p_{3/2}$ peak centered at 933.4 eV with the presence of a small satellite peak at 944.3 eV was assigned to CuO.[18−22] In addition, a further Cu $2p_{2/3}$ peak at around 935.4 eV indicates the possible presence of $Cu(OH)_2$.[15] The $Cu(OH)_2$ and CuO species appeared in the Cu/zeolite sample synthesized by a hydrated process.[18,19] The freshly prepared Cu/ZSM-5 zeolite adsorbent has more CuO (57.3%) and less $Cu(OH)_2$ (42.7%). Besides, the intensity ratio of the accompanying Cu 2p satellite was only 6−8% in Cu/ZSM-5 zeolite adsorbent before adsorption. After adsorption and air purging, it was observed that the relative percentage of $Cu(OH)_2$ (54.4%) becomes more than that of CuO (45.6%). Also, the ratios of Cu 2p satellite intensities were increased to 33−38%, values much higher than those before adsorption.

A test has also been done on the reuse of Cu/ZSM-5 adsorbent for PH_3 removal after air purging of the exhausted adsorbent for 30 min. The result revealed that PH_3 removal efficiencies of up to 97% were achievable for the regenerated adsorbent; it then gradually decayed after around 8 min. The maximal PH_3 removal efficiency of 97% could not reach the goal of 99%;

hence the result is not shown. However, this still proved that regeneration of the adsorbent should be possible, but a better regeneration process has to be found for complete recovery of the Cu/ZSM-5 adsorbent.

4. Conclusions

A PH_3 adsorption efficiency of >99% using Cu/zeolite adsorbents was achieved with a PH_3 inlet concentration of 10 000 ppmv. The specific surface area had a minimal effect on the PH_3 adsorption when Cu/ZSM-5 zeolite was used, but it could govern the PH_3 adsorption when Cu/Y zeolite was used. The optimal Cu loaded amount for achieving the highest PH_3 adsorption capacity of around 30 mg of PH_3/g of adsorbent is about the same at around 3−4% for both Cu/ZSM-5 and Cu/Y zeolites. To achieve this maximum PH_3 adsorption capacity, ZSM-5 zeolite requires a much higher $Cu(NO_3)_2$ precursor concentration (∼5 mol/L) while it is much lower (∼1 mol/L) for the Y zeolite.

The results also showed that CuO is the major species on the ZSM-5 zeolite adsorbent before PH_3 adsorption, while $Cu(OH)_2$ becomes the major species after PH_3 adsorption and air purging. Further studies should be directed toward detailed discussion on the Cu status that can enhance the PH_3 adsorption capacity as well as the preparation of active Cu with high specific surface area. The regeneration of the Cu zeolite adsorbent for reducing hazardous waste disposal is also an interesting research subject that has practical application potential.

Literature Cited

(1) Colabella, J. M.; Stall, R. A.; Sorenson, C. T. The Adsorption and Subsequent Oxidation of AsH_3 and PH_3 on Activated Carbon. *J. Cryst. Growth* **1988**, *92*, 189.

(2) Hardwick, S. J.; Mailloux, J. C. Waste Minimization in Semiconductor Processing. *Mater. Res. Soc.* **1994**, *344*, 273.

(3) Leondaridis, P.; Vendel, A. S.; Akthar, T. Removal of gaseous hydrides. U.S. Patent 5,182,088, 1993.

(4) Cotton, M. L.; Johnson, N. D.; Wheeland, K. G. Removal of Arsine from Process Emissions. *Metall. Soc. CIM* **1977**, Annu. Vol. Featuring Molybdenum, 205.

(5) Haacke, G.; Brinen, J. S.; Burkhard, H. Arsine Adsorption on Activated Carbon. *J. Electrochem. Soc.* **1988**, *135*, 715.

(6) Tsai, W. T. A Review of Environmental Hazards and Adsorption Recovery of Cleaning Solvent Hydrochlorofluorocarbons (HCFCs). *J. Loss Prevent. Process Ind.* **2002**, *15*, 147.

(7) Monneyron, P.; Manero, M.-H.; Foussard, J.-N. Measurement and Modeling of Single- and Multi-compound Adsorption Equilibria of VOC on High-Silica Zeolites. *Environ. Sci. Technol.* **2003**, *37*, 2410.

(8) Chintawar, P. S.; Greene, H. L. Adsorption and Catalytic Destruction of Trichloroethylene in hydrophobic zeolites. *Appl. Catal., B* **1997**, *14*, 37.

(9) Chang, F. T.; Lin, Y. C.; Bai, H.; Pei, B. S. Adsorption and Desorption Characteristics of Semiconductor Volatile Organic Compounds on the Thermal Swing Honeycomb Zeolite Concentrator. *J. Air Waste Manage. Assoc.* **2003**, *53*, 1384.

(10) Lucas, D.; Valverde, J. L.; Dorado, F.; Romero, A.; Asencio, I. Influence of the Ion Exchanged Metal (Cu, Co, Ni and Mn) on the Selective Catalytic Reduction of NOx over Mordenite and ZSM-5. *J. Mol. Catal. A: Chem.* **2005**, *225*, 47.

(11) Baek, S. W.; Kim, J. R.; Ihm, S. K. Design of Dual Functional Adsorbent/Catalyst System for the Control of VOC's by using Metal-loaded Hydrophobic Y-zeolites. *Catal. Today* **2004**, *93*−*95*, 575.

(12) Yahiro, H.; Iwamoto, M. Copper Ion-exchanged Zeolite Catalysts in DeNOx Reaction. *Appl. Catal., A* **2001**, *222*, 163.

(13) Berthomieu, D.; Delahay, G. Recent Advances in Cu(I/II)Y. *Catal. Rev.* **2006**, *48*, 269.

(14) Meier, W. M.; Olson, D. H. *Altas of Zeolite Structure Types*, 3rd revised ed.; Butterworth-Heinemann: Woburn, MA, 1992.

(15) Kundakovic, L.; Stephanopoulos, M. F. Deep Oxidation of Methane over Zirconia Supported Ag Catalysts. *Appl. Catal., A* **1999**, *183*, 35.

(16) Quinn, R.; Dahl, T. A.; Diamond, B. W.; Toseland, B. A. Removal of Arsine from Synthesis Gas Using a Copper on Carbon Adsorbent. *Ind. Eng. Chem. Res.* **2006**, *45*, 6272.

(17) Hsu, J.-N.; Tsai, C.-J.; Chiang, C.; Li, S.-N. Silane Removal at Ambient Temperature by Using Alumina-Supported Metal Oxide Adsorbents. *J. Air Waste Manage. Assoc.* **2007**, *57*, 203.

(18) Narayana, M.; Contarini, S.; Kevan, L. X-ray photoelectron and electron spin resonance spectroscopic studies of Cu-NaY zeolites. *J. Catal.* **1985**, *94*, 370.

(19) Contarini, S.; Kevan, L. X-ray photoelectron spectroscopic study of copper-exchanged X-and Y-type sodium zeolites: resolution of two cupric ion components and dependence on dehydration and x-irradiation. *J. Phys. Chem.* **1986**, *90*, 1630.

(20) Shpiro, E. S.; Grünert, W.; Joyner, R. W.; Baeva, G. N. Nature, distribution and reactivity of copper species in over-exchanged Cu-ZSM-5 catalysts: and XPS/XAES study. *Catal. Lett.* **1994**, *24*, 159.

(21) Robert, T.; Offergeld, G. X-ray Photoelectron Spectra of Solid Copper. Compounds. Relation between the Presence of Satellite Lines and the State of Oxidation of Copper. *Phys. Status Solidi A* **1972**, *14*, 277.

(22) Robert, T.; Bartel, M.; Offergeld, G. Characterization of O Species Adsorbed on Copper and Nickel Oxides by X-Ray Photo-Electron Spectroscopy. *Surf. Sci.* **1972**, *33*, 123.

Received for review August 7, 2007
Revised manuscript received November 21, 2007
Accepted November 21, 2007

IE071074N